Positron annihilation and broadband dielectric spectroscopy: A series of propylene glycols

J. Bartoš [a,*], O. Šauša [b], M. Köhler [c], H. Švajdlenková [a], P. Lunkenheimer [c], J. Krištiak [b], A. Loidl [c]

[a] Polymer Institute of SAS, Dúbravská cesta 9, SK-842 36 Bratislava, Slovak Republic
[b] Institute of Physics of SAS, Dúbravská cesta 9, SK-842 28 Bratislava, Slovak Republic
[c] Experimental Physics V, Center for Electronic Correlations and Magnetism, University of Augsburg, D-86135 Augsburg, Germany

1. Introduction

The basic topic of glass science is the physical nature of the slowing-down of molecular motion when approaching the liquid to glass transition at the glass temperature, T_g.This issue is addressed by a variety of experimental techniques, theories and simulations [1,2]. Structural methods such as X-ray diffraction and neutron scattering indicate no dramatic change in the disordered arrangement of the molecules, in both the liquid and glassy states of amorphous phase [3]. However, thermodynamic and especially, dynamic methods such as neutron scattering (NS), broadband dielectric spectroscopy (DS), nuclear magnetic resonance (NMR) and electron spin resonance (ESR) strongly point to the existence of close connections of the glass transition to an evolution of the structural relaxation dynamics of glass-formers from the low viscosity (rapidly relaxing) liquid towards the solid (very slowly relaxing) glass [4].

In structural glass-formers, several dynamic regimes over a wide temperature interval are found ranging from the normal liquid state through the supercooled liquid one towards the glassy state. They are marked by various characteristic temperatures, e.g., the Arrhenius T_A [5,6], Stickel T_B^{ST}[7], Alegría $T_B^{\beta_{KWW}}$ [8] and Schönhals T_B^{SCH} temperature [9]. The physical origin of these dynamically distinct regions and the closely related crossover temperatures is the subject of intense multi-methodical research and evidently, their explanation can significantly help to achieve a better understanding of the liquid–glass transition process.

The search for possible relationships between structural and dynamic parameters in disordered materials as one possible explanation for the above-mentioned problem is a rather challenging problem and such an effort did not lead to straightforward results until now. The structural-dynamic state of glass-formers is often treated in terms of a simple and physically plausible free volume concept serving as a measure of the structural disorder or/and the mobility of the constituents of condensed material which became very useful in the interpretation of the thermodynamic, dynamic and transport properties [10,11]. In this context, PALS as a special structure-dynamic sensitive method, is of high relevance. It detects static and dynamic regions of reduced electron density, so-called free

* Corresponding author. Tel.: +421 2 54 77 34 48; fax: +421 2 54 77 59 23.
E-mail address: upolbrts@savba.sk (J. Bartoš).

volumes. The PALS technique is based on the annihilation behavior of the atomistic ortho-positronium (o-Ps) probe, i.e. a bound system of a positron and electron. This method is an effective tool for the free volume characterization of ordered and especially, of disordered condensed materials [12–14]. The positron and especially the o-Ps probe act as a very sensitive indicator of the presence of static (permanent) and dynamic (transient) free volumes such as quasi-static vacancies in real crystals or free volume holes in the amorphous phase. The ortho-positronium (o-Ps) lifetime, τ_3, is a measure of the size of these structure defects or free volume regions [15].

In crystalline systems, the o-Ps lifetime, as a function of temperature $\tau_3(T)$, exhibits two distinct regions corresponding to the ordered (crystal) and disordered (liquid) phase, with a sharp step effect at the melting temperature, T_m [16]. On the other hand, amorphous small-molecule and polymeric glass-formers show a typical sigmoidal or quasi-sigmoidal dependence of $\tau_3(T)$ extended over a more or less wide temperature range and finished by a pronounced plateau or quasi-plateau effect at higher temperatures with respect to T_g [17]. Phenomenological analyses of the $\tau_3(T)$ plots indicate several regions that show linear behavior, marked by the characteristic PALS temperatures, which, according to a unified notation [18], are depicted as T_g^{PALS}, T_{b1} and $T_{b2}=T_r=T_k$ [19]. The two latter temperatures are situated at $T_{b1}\cong(1.2-1.4)T_g^{PALS}$ [18,20] and $T_{b2}\cong(1.4-1.7)T_g^{PALS}$ [17–19], respectively.

The complete structure-dynamic characterization of any disordered substance by PALS over a wide temperature range requires understanding the origin of these different regions and the closely related characteristic PALS temperatures. To achieve this goal, they may be compared with the characteristic temperatures detected by more traditional techniques indicating thermodynamic or dynamic changes. At present, certain relations between various features of the PALS response and those in viscosity [5,19] or dielectric spectra [6–9,21–24] seem to suggest to some extent a dynamic character of the PALS response in the liquid state of glass-formers. In 1980 Pethrick [19] discovered that an onset of the quasi-plateau feature in the PALS response at $T_{b2}=T_r$ is situated close to the Arrhenius temperature, T_A, above which the structural, i.e., viscosity [5,19] or α-relaxation [6,21,22] dynamics occur approximately in the thermally activated fashion. Recent advances in broadband dielectric spectroscopy (BDS) [21,22] enabled to reveal further connections between the PALS response and the glassy dynamics [23–25]. In particular, the two often observed empirical T_{b2} and T_{b1} rules provide information about the specific relationships between the o-Ps lifetime, τ_3, and the primary α relaxation time, τ_α, namely, $\tau_\alpha(T_{b2})\sim10^{-9}$ s or $\tau_\alpha(T_{b1})\sim10^{-6\pm1}$ s, respectively [18,23]. In the former case, for many glass-formers at the onset of the plateau or quasi-plateau effect in the PALS response the relation $\tau_3=\tau_\alpha$ has been often found. Sometimes, T_{b2} lies in the vicinity of the characteristic Stickel, T_B^{ST}, or Schönhals, T_B^{SCH}, temperature, while in other cases, rather T_{b1} is situated close to the characteristic Stickel T_B^{ST} temperature [23–25]. The latter finding seems to suggest a certain role of the primary process for the PALS response, but also some indications about a possible role of the slow secondary relaxations in a few small molecular glass-formers were suggested [24,25]. In summary, at the present time, the empirical situation is still incomplete and requires further combined and systematic investigations.

In this contribution, we present detailed phenomenological analyses of the response obtained from measurements by dielectric spectroscopy and PALS of a series of amorphous glass-formers, namely, the above-mentioned propylene glycols (PGs). This combined approach reveals new connections between the o-Ps annihilation and the spectral and relaxation characteristics of dipolar relaxation, especially in the supercooled liquid state. This underlines a close relationship between both the PALS and BDS responses and points to the dynamic character of the PALS response.

2. Experimental

2.1. Materials

Propylene glycol (PG), dipropylene glycol (DPG) and tripropylene glycol (TPG), having the structural formula HO–[CH_2–CH (CH_3)–O]$_n$–H with $n=1$, 2 and 3, were purchased from Aldrich and Fluka and used as received. Glass transition temperatures were determined by differential scanning calorimetry (DSC) using a Perkin-Elmer DSC Pyris 1 with heating rate of 10 K/min.

2.2. PALS method

Positron annihilation lifetime spectra of the series of propylene glycols (PG's) were obtained at the Institute of Physics of SAS, Bratislava by the conventional fast–fast coincidence method using plastic scintillators coupled to Phillips XP2020 photo-multipliers. The time resolution of prompt spectra was about 320 ps. The radioactive positron ^{22}Na source and the sample assembly were kept under vacuum in a cryogenerator. During the low-temperature measurements from 15 K up to 300 K, the samples were mounted in a holder at the end of a cold finger of a closed-cycle refrigerator from Leybold with an automatic temperature regulation. Measurements at temperatures above room temperature were performed in a chamber without vacuum. The stability of the temperature was about 1 K [26]. The positron lifetime spectra were analyzed using the well-known PATFIT-88 software package [27] in terms of a short-term component from para-positronium p-Ps, τ_1, an intermediate one attributed to "free" positron, τ_2, and a long-term one, related to free volume: ortho-positronium o-Ps, τ_3. The acquisition time was at least 2 h for each temperature.

2.3. BDS methods

Broadband dielectric measurements of the same PG's samples have been performed at the University of Augsburg using a combination of different techniques enabling to cover nearly 20 decades in frequency [21,28–32]. In the low-frequency range a frequency response analyzer (Novocontrol α-analyzer, 10^{-3} Hz$<\nu<$10 MHz) and an autobalance bridge (HP4284, 20 Hz–1 MHz) were used. For the radio-frequency and microwave range (1 MHz$<\nu<$3 GHz), a reflectometric technique was employed, with the sample capacitor mounted at the end of a coaxial line [31]. These measurements were performed with the HP4291 and HP4991 impedance analyzers. For all the above-mentioned methods, the sample material was filled into parallel-plate capacitors. In the region 100 MHz–25 GHz coaxial transmission measurements using the HP8510 network analyzer were carried out [28]. These measurements require filling the sample material into a specially designed coaxial line, sealed with Teflon discs. At frequencies 60 GHz$<\nu<$1.2THz, a quasi-optical sub-millimeter spectrometer [32] was used with an experimental arrangement similar to a Mach–Zehnder interferometer (for more details, see Refs. [28,32]). For temperature variation and N_2-gas cryostats were used.

3. Results

3.1. PALS data

Fig. 1 displays the o-Ps lifetime, τ_3, as a function of the temperature, T, for all the three PG samples as obtained over very wide temperature ranges from 15 K up to 330 K–390 K. Several features and trends can be seen. The τ_3–T plots reveal a typical quasi-sigmoidal shape and seem to exhibit four different regions with rather distinct thermal behavior, separated by three changes of slope (marked by I–IV in Fig. 1). A high-temperature plateau shows up, which seems to display some fine structure being more pronounced for the higher

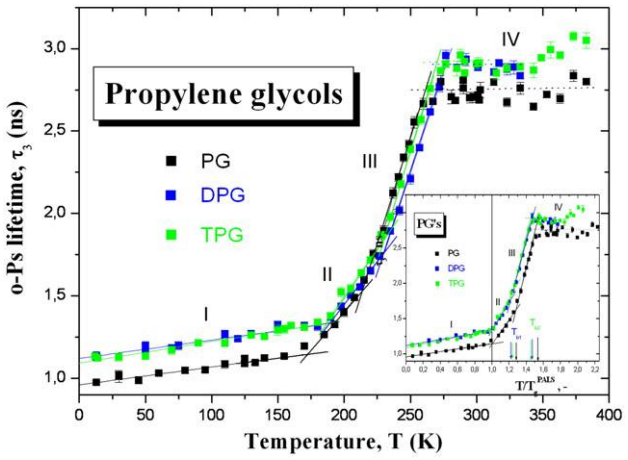

Fig. 1. o-Ps lifetime, τ_3, as a function of the absolute temperature, T, and of the normalized temperature T/T_g^{PALS}(inset) for a series of PG's. The lines are linear fits with the fitting parameters from Table 1.

members of the PG series. In addition, the absolute value of the τ_3- in the low-T region is higher for the di- and trimer, which, however, both are of similar magnitude. In the temperature region between the low and high regions, the annihilation times show two linear regimes. Especially in region II, the τ_3 values of all three PG's approach each other while at the highest temperatures the same order of the τ_3 values as for the lowest ones is observed. A phenomenological analysis of the above-mentioned four regions in the PALS response by linear fitting [18,20] reveals the characteristic PALS temperatures: T_g^{PALS}, T_{b1} and finally, T_{b2}. The fitting parameters are provided in Table 1.

The intersection temperature of the first pronounced bend effect in the low-temperature region defines the PALS glass transition temperature, T_g^{PALS}. It was determined from a phenomenological analysis of the τ_3–T plot for each propylene glycol, leading to: $T_g^{PALS} = 172$ K for PG, $T_g^{PALS} = 189$ K for DPG and finally, $T_g^{PALS} = 186$ K for TPG. These values are acceptable agreement to the glass transition temperatures from thermodynamical and dynamic studies such as differential scanning calorimetry T_g^{DSC} and dielectric spectroscopy T_g^{DS} [33] — see Table 2. The latter values are consistent with the first systematic low-frequency study of a series of PG's [34].

In addition to T_g^{PALS}, two further characteristic PALS temperatures situated in the liquid state are found: T_{b1} and T_{b2}. The corresponding values of both characteristic PALS temperatures in the liquid state for PG, DPG and TPG are $T_{b1} = 218$ K, 232 K or 231 K, respectively. For the sake of simplicity, only the initial part of the high-temperature plateau was considered for estimation of the respective values of T_{b2} leading to ~263 K, 277 K and 272 K.

3.2. BDS data

Fig. 2 shows the broadband dielectric spectra as a function of frequency at various temperatures for PG, DPG and TPG [33]. The dielectric response of the di- and trimer is of different type in the low-temperature region than that of the monomer. According to the classification scheme by Kudlik et al. [35], propylene glycol (PG) is a Type A glass-former exhibiting only α-peak in the spectra without any secondary peak. Instead, the so-called excess wing (EW), i.e. a second power law at the high-frequency flank of the α-peak is observed. The latter can be ascribed to a submerged slow secondary relaxation [36–38]. On the other hand, the dimer and trimer are typical Type B glass-formers as at frequencies beyond the α-relaxation process a secondary relaxation peak shows up [39]. However, above 220–230 K, both the peaks merge and at highest temperatures the spectra of all three glycols exhibits rather similar characteristics. Finally, at still higher frequencies, a minimum is present in the imaginary part of the dielectric loss. Additional contributions in this region evidence a fast process, the so-called fast β-process caused by the rattling motion of the molecules in their cages [21,40].

Table 2
Comparison between the glass transition temperatures from PALS with those from thermodynamic [33] and dynamic [33] methods in a series of PG's.

System	T_g^{PALS}	T_g^{DSC}	$T_g^{DS}(\tau_\alpha = 10^2 s)$
PG	172	170	166
DPG	189	196	193
TPG	186	194	189

The primary and slow secondary relaxations in various propylene glycols were extensively studied in several papers but these studies covered rather the lower frequency range [34,39–42]. On the basis of special aging [36] and pressure experiments [41,42] it was concluded that while in the *PG* the excess wing can be identified with a slow secondary relaxation, for the dimer and trimer even two secondary peaks can be distinguished in the DS spectra [40–42]. In addition to the intense second faster secondary peak, the first minor and slower secondary peak is visible only in the vicinity of the respective $T_g^{DS}(\tau_\alpha = 10^2 s)$[41,42]. Then, the slower secondary process in all the PG's is postulated to be of Johari–Goldstein (JG) type [43] and the faster secondary process in the DPG, and TPG is marked as a γ-peak and considered to be of non-JG type [44]. This aspect has already been discussed by some of us in Ref. [33].

To obtain the spectral and relaxation parameters of the individual relaxation modes in all the PG's, the BDS spectra can be analyzed in terms of the Cole–Davidson (CD) [45] and Cole–Cole (CC) [46] function for the primary α process or for the secondary processes in PG, DPG and TPG, respectively. Then, the two main relaxation features of the BDS spectra are deconvoluted assuming an additive scheme using the following expression:

$$\varepsilon'' = \mathrm{Im}\left[\frac{\Delta\varepsilon_{CD}}{(1+i\omega\tau_{CD})^{\beta_{CD}}} + \frac{\Delta\varepsilon_{CC}}{1+(i\omega\tau_{CC})^{1-\alpha_{CC}}}\right] + \varepsilon_c \qquad (1)$$

Here, $\Delta\varepsilon_{CD}$ and $\Delta\varepsilon_{CC}$ are the relaxation strengths, τ_{CD} and τ_{CC} the relaxation times, and β_{CD} and α_{CC} the spectral width parameters of the CD and CC function, respectively and ω is the circular frequency.

The mean relaxation times of the primary α process, $\tau_\alpha = \tau_{CD}\beta_{CD}$, in all the PG's are plotted in Fig. 3 as a function of the absolute temperature. In general, their course exhibits non-Arrhenius character with a crossover towards an Arrhenius regime at higher temperatures — see

Table 1
Fitting parameters of the linear expressions of a form $\tau_3 = aT + b$ for regions I–III in the series of PG's.

System	Region I		Region II		Region III	
	$a\times10^3$, ns/K	b, ns	$a\times10^2$, ns/K	b, ns	$a\times10^2$, ns/K	b, ns
PG	1.09 ± 0.09	0.96 ± 0.01	0.98 ± 0.08	−(0.56 ± 0.16)	2.78 ± 0.17	−(4.49 ± 0.41)
DPG	1.12 ± 0.06	1.12 ± 0.01	1.02 ± 0.09	−(0.59 ± 0.18)	2.44 ± 0.05	−(3.87 ± 0.14)
TPG	1.30 ± 0.07	1.09 ± 0.01	1.17 ± 0.06	−(0.85 ± 0.12)	2.60 ± 0.13	−(4.13 ± 0.32)

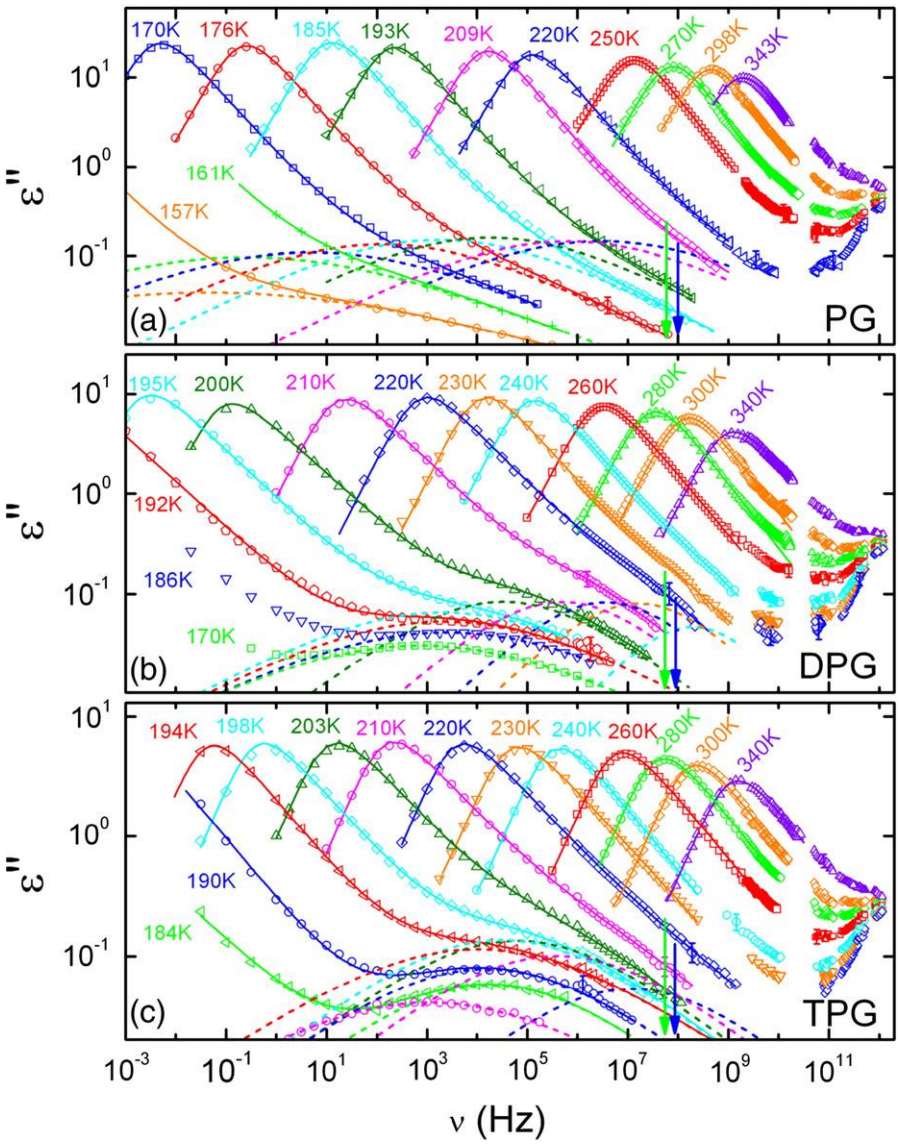

Fig. 2. Spectral evolution of dielectric loss in a series of PG's [33]. The equivalent frequencies $f_3(T_{b1})$ and $f_3(T_{b2})$ are also included showing their relationships to the high-frequency tail of the primary α-peak or to the maximum of the primary α-peak, respectively. The solid lines represent the total fitting using the additive scheme of Eq. (1) and the dashed lines are the secondary process contributions.

also Fig. 5 below. Phenomenologically, the temperature dependence of τ_α can be described in several ways and one relatively novel of them will be discussed later.

Fig. 4 presents the temperature dependence of the relaxation times of the secondary process in PG, DPG and TPG over a wide temperature range including also the glassy state below $T_g^{DS}(\tau_\alpha = 10^2 s)$. The secondary relaxation time in *PG* exhibits slight deviations from Arrhenius behavior, while DPG and TPG show a complicated character, namely a shallow minimum close to T_g^{DS} in agreement with Refs. [42,47]. Importantly, the secondary relaxation times in all the PG's samples above T_g^{DS} follow non-Arrhenius behavior and approach each other with increasing temperature suggesting rather a similar origin [33].

The other spectral and relaxation parameters of the structural relaxation, i.e. relaxation strength and spectral width parameters are presented below in an alternative phenomenological analysis of the dielectric data in terms of the modified Vogel–Fulcher–Tamman–Hesse (M-VFTH) equation within the two-order parameter (TOP) model.

4. Discussion

4.1. Phenomenological relationships between the PALS response and the BDS data

In the following we present a detailed comparison of the PALS response with the spectral evolution of the dielectric loss and their relaxational and spectral parameters, i.e. time scales, fragilities, relaxation strengths and spectral widths.

First of all, for discussion of the correct trends in the PALS and BDS properties with molecular weight M, we rescaled Figs. 1 and 3 by the respective T_g's for all the PG's.

The inset of Fig. 1 shows the o-Ps lifetime, τ_3, as a function of the normalized temperature, T/T_g^{PALS}. Similar PALS results have been obtained in Ref. [48], but the data covered significantly narrower ranges with an essentially larger temperature step which prevents to reveal some detailed features. In this representation, the τ_3 values for PG are systematically lower than those for the remaining members of the PG family over the whole temperature range studied. This could

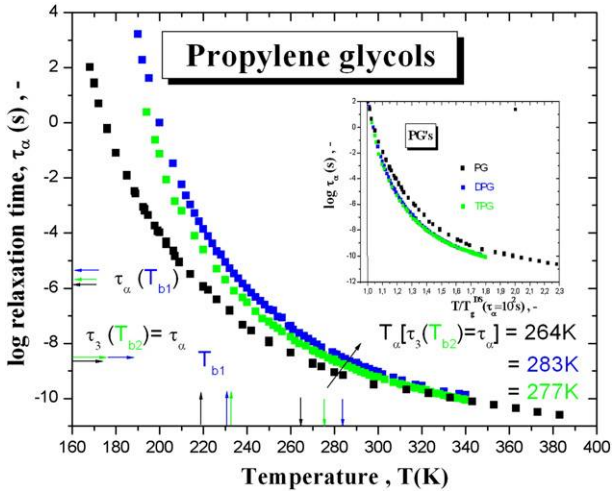

Fig. 3. Mean primary α relaxation times as a function of the absolute temperature and of the T_g^{DS} normalized temperature (inset) for all the PG's [33]. The arrows mark: i) the o-Ps lifetimes at T_{b2} and the corresponding identity α temperature T_α supporting the T_{b2} rule and ii) the average primary α relaxation times at T_{b1} demonstrating the validity of the T_{b1} rule — see text.

be expected on the basis of the higher content of OH-groups in the monomer and its higher tendency to form the intermolecular H-bonds resulting into the more compact packing of the molecules in the PG matrix. The temperature dependences of the o-Ps lifetime, normalized by the corresponding T_g's for the dimer and trimer are rather similar with slightly higher values for the latter. This is probably due to a fine interplay between the decreasing H-bonding extent and the increasing chain character of the entities on going from DPG to TPG. These opposite factors could result also in the inverse order in the corresponding PALS glass transition temperature.

The relative characteristic PALS temperatures for the series of the three PG's $T_{b1}/T_g^{PALS} = 1.27, 1.23$ and 1.24 and $T_{b2}/T_g^{PALS} = 1.53, 1.47$ and 1.46 fall into the typical ranges as found by us [18,23] as well as by other authors [17,19,20], namely, $T_{b1} \in (1.2–1.4)\ T_g^{PALS}$ and $T_{b2} \in (1.4–1.7)\ T_g^{PALS}$. Thus, all the PG's behave consistent with the majority of small-molecule and polymer glass-formers studied so far. Note that some exceptions of these empirical rules, especially for very fragile glass-formers, have been observed [49]. This deserves further attention in future studies.

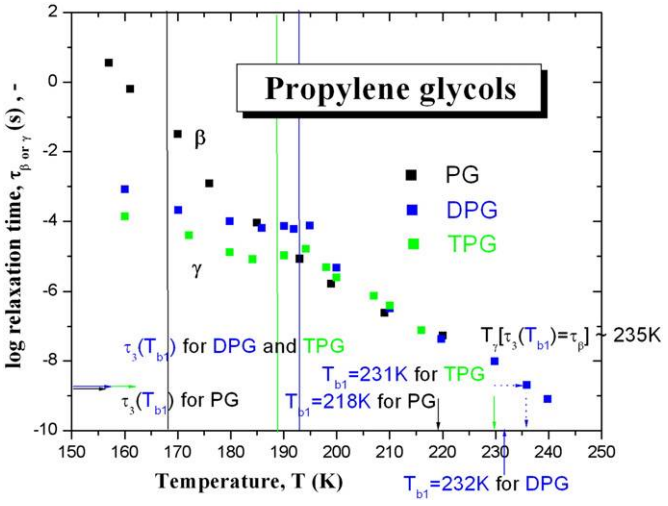

Fig. 4. Temperature dependences of the slow secondary relaxation time for PG, DPG and TPG. The arrows mark the o-Ps lifetimes at the respective T_{b1}'s for all the PG's and in the case of DPG the identity β temperature T_β revealing the mutual relationship between the time scales of the o-Ps annihilation and the secondary process. The vertical lines indicate the corresponding $T_g^{DS}(\tau_\alpha = 10^2 s)$values.

The inset of Fig. 3 displays the average relaxation times of the primary α process as a function of temperature normalized to T_g. At the same relative T/T_g^{DS}, the slowest primary α process is observed in the highly H-bonded PG and it is accelerated on crossing to DPG and TPG. The latter two follow the same order with rather close temperature dependences in consistency with the PALS response in the inset of Fig. 1.

As already mentioned, the PALS spectra of all investigated propylene glycols exhibit basically four regions of the distinct thermal behavior of the o-Ps lifetime vs. temperature, which are characterized by the corresponding temperature variations of the o-Ps lifetime as well as by the three characteristic PALS temperatures: T_g^{PALS}, T_{b1} and T_{b2}. From Table 1 it becomes obvious that the variation of the o-Ps lifetime with temperature, $\beta_{\tau 3} = (\Delta\tau_3/\Delta T)$, increases with molecular weight, M, of the PG matrix both in the glassy state as well as in the *deeply* supercooled liquid state. For the latter case, the order of the temperature variation of the o-Ps lifetime follows an increasing trend with fragility, $m_g = 48, 69$ and 74 for PG, DPG and TPG taken from [33]. Similar behavior was revealed previously by some of us for a series of polymers [50], i.e., the fragility grows with increasing temperature variation of the o-Ps lifetime of the *deeply* supercooled liquid. On the other hand, in the *slightly* supercooled liquid, $\beta_{\tau 3}$ exhibits generally a decreasing trend with a local minimum for DPG.

Next, we will further analyze the PALS and BDS responses of the propylene glycols individually.

4.1.1. Propylene glycol (PG)

The PALS response of PG as measured over an extraordinary wide temperature range from 15 K up to 380 K is displayed in the T and T_g^{PALS} normalized representations in Fig. 1. Here, we can observe an onset of a rapid increase in the o-Ps lifetime at the first characteristic PALS temperature $T_g^{PALS} \sim 172$ K followed by the slighter bend effect at the first characteristic liquid PALS temperature $T_{b1} = 218\ \text{K} = 1.27\ T_g^{PALS}$and finally, finished by a dramatic crossover towards the plateau level at the second characteristic liquid PALS temperature $T_{b2} = 263\ \text{K} = 1.53\ T_g^{PALS}$ — see also ref. [23].

As already mentioned, the BDS spectra of PG were analyzed with the sum of a CD and a CC function accounting for the primary α relaxation and the excess wing, the latter being identified as the submerged β relaxation – see Fig. 2a. Good fits of the dielectric loss spectra were achieved by including the CC term up to 220 K. On the other hand, the $\varepsilon''(\nu)$ spectra are fitted for $T > 220$ K with the CC term set to zero [33]. This finding seems to give some hint on the origin of the slighter change of the slope of the PALS response at $T_{b1} = 218$ K in Fig. 1. Figs. 3 and 4 show the relaxation map of the PG sample summarizing the relaxation times of all the dynamic processes, i.e. the primary α and the secondary β process together with the corresponding o-Ps lifetimes at both characteristic PALS temperatures $\tau_3(T_{b1})$ and $\tau_3(T_{b2})$. Although the β peak is detectable at T_{b1}, the so-called identity β temperature, i.e. the temperature, at which the o-Ps lifetime $\tau_3(T_{b1})$ equals the secondary β relaxation time, τ_β, $T_\beta[\tau_3(T_{b1}) = \tau_\beta]$ cannot be determined because of almost the one order of magnitude difference between the PALS and BDS time scales: $\tau_\beta(T_{b1}) = 5.4 \times 10^{-8}$ s vs. $\tau_3(T_{b1}) = 1.7 \times 10^{-9}$ s. This finding is based on the β peak maximum and at first glance seems to suggest rather the absence of a direct connection between the slighter bend effect in the PALS response at T_{b1} and the slow secondary β relaxation. However, the β peak is very broad implying a broad distribution of the β relaxation times [22], so that some contribution from the faster part of this distribution cannot be excluded. Indeed a simple inspection of Fig. 2 reveals that the β-relaxation most likely plays a role in the generation of the change of slope at T_{b1}: At high temperatures, $T > T_{b1}$, the response for $\nu = 1/[2\pi\tau_3(T_{b1})] \approx 90$ MHz obviously is dominated by the α-relaxation (see, e.g., the curve at 250 K in Fig. 2(a)). However, with decreasing

temperature at this frequency the excess wing (i.e. the submerged secondary relaxation) starts to govern the loss somewhere in the region between 220 and 209 K, which nicely agrees with the value of $T_{b1} = 218$ K found in the PALS experiment.

In our search for the origin of further dynamic processes which could be responsible for the T_{b1} effect, it is useful to recall the T_{b1} rule, i.e., $\tau_\alpha(T_{b1}) \cong 10^{-6\pm1}$ s which is well satisfied for PG as it is evident from Fig. 3. Similarly, this T_{b1} rule was found to be valid for many small molecular and polymer glass-formers [18,23]. In spite of the approximately 3 ± 1 decade difference between the relevant time scales of the o-Ps lifetime and the *average* α relaxation times, this rule seems to suggest that the slighter bending in the PALS response at T_{b1} in some way may be related to the primary α relaxation process. In light of the above-mentioned transition from α-peak dominated to secondary relaxation dominated response, the T_{b1} rule found to be valid in many glass-formers seems to suggest a close relation of α- and secondary relaxation or of α-relaxation and excess wing. Most likely this universal behavior can be explained by one of the various concepts assuming a close connection of alpha and secondary relaxation/excess wing, e.g. the Nagel scaling [51] or Ngai's extended coupling model [52].

At even higher temperatures, a very pronounced plateau effect in the PALS response of the PG sample at the second characteristic liquid PALS temperature, $T_{b2} = 263$ K is found. From Fig. 3 it follows that the so-called identity α temperature $T_\alpha[\tau_3(T_{b2}) = \tau_\alpha]$, i.e. the temperature, at which $\tau_\alpha(T)$ reaches the o-Ps lifetime τ_3, being 264 K, agrees with the plateau temperature $T_{b2} = 263$ K. This empirical finding is a further confirmation of the T_{b2} rule, found previously for many small molecular and polymer glass-formers by us as well as by others [17–19]. Moreover, this empirical finding can be also related to the Schönhals temperatures $T_B^{SCH} = 268$ K which marks a dramatic change in the structural relaxation indicating a crossover from a low-temperature (highly cooperative) to a high-temperature (slightly cooperative or non-cooperative) dynamic regime [9,23]. To identify the physical mechanism responsible for this drastic change in the PALS response as well as the crossover in the structural relaxation, it is interesting to mention recent findings of one of us from an atomistic modeling of the bulk PG system via a combination of molecular dynamics (MD) simulation and cavity analysis (CAVA) [53]. It was revealed that the *static* free volume accessible to the o-Ps probe is percolated over the whole many-particle system just in the vicinity of the plateau PALS temperature T_{b2}. This free volume percolation should lead to the facilitation of the non-cooperative structural dynamics at higher *T*'s. All these PALS, BDS and MD + CAVA findings taken together seem to be consistent with the qualitatively different, i.e., *liquid*-like character of the low viscosity, i.e., normal *PG* liquid at relatively higher temperatures with respect to the glass transition temperature.

4.1.2. Dipropylene glycol (DPG)

The temperature dependent PALS response of the DPG measured over an extraordinary wide temperature range from 18 K up to 330 K is presented in Fig. 1. The inset shows the data normalized with respect to T_g^{PALS}. The o-Ps lifetimes behave similarly as in the monomer. The onset of the more rapid increase in the o-Ps lifetime is observed at the first characteristic PALS temperature $T_g^{PALS} = 189$ K followed by the weaker change of slope at the first characteristic liquid PALS temperature $T_{b1} \sim 232\ \text{K} = 1.23\ T_g^{PALS}$ and finally, finished by a dramatic crossover towards the plateau level at the second characteristic liquid PALS temperature $T_{b2} \sim 277\ \text{K} = 1.47\ T_g^{PALS}$. These relative PALS temperatures are lower than in the monomer PG. This signifies a decrease of these temperatures for the higher fragility of DPG ($m_g = 69$) compared to PG ($m_g = 48$) [33].

DPG as a representative of Type B glass-formers exhibits a well pronounced peak, ascribed to a secondary process [41,42]. The BDS spectra of DPG were analyzed with the sum of a CD and a CC function for the primary α relaxation or the slow secondary relaxation, respectively — see Fig. 2b. Similarly as in the previous PG case, good fits of the BDS spectra in the liquid states could be achieved by including the CC term for $T \leq 240$ K. As mentioned before, at $T > 240$ K the BDS spectra can be satisfactorily fitted when the CC term is neglected [33]. This finding seems also to be related to the slight change of slope in the PALS response at $T_{b1} \sim 232$ K in Fig. 1.

In Figs. 3 and 4 the relaxation times of the primary α- and the secondary β-processes are plotted together with the corresponding o-Ps lifetimes at both the characteristic PALS temperatures $\tau_3(T_{b1})$ and $\tau_3(T_{b2})$. The secondary peak is still detectable at T_{b1} and moreover, the so-called identity β temperature, $T_\beta[\tau_3(T_{b1}) = \tau_\beta]$, i.e., the temperature at which the o-Ps lifetime $\tau_3(T_{b1})$equals the secondary β relaxation time, τ_β. The T_β value could be estimated by an interpolation, 235 K being close to $T_{b1} = 232$ K. This is consistent with the spectral evolution, where $f_3(T_{b1})$ falls in between the two neighbored secondary peaks at 230 K and 240 K — Fig. 2b. This agreement indicates a *direct* connection between the slight bend effect at T_{b1} in the PALS response and this secondary relaxation as discussed in detail for the monomer in the previous sections. Similarly to PG, the T_{b1} rule, i.e., $\tau_\alpha(T_{b1}) \cong 10^{-6\pm1}$ s is also satisfied for DPG — see Fig. 3.

On further increase the temperature, the PALS response of the DPG sample develops into a very pronounced plateau effect characterized by the second characteristic liquid PALS temperature, $T_{b2} = 277$ K — Fig. 1. From Fig. 3 it follows that the so-called identity α temperature $T_\alpha[\tau_3(T_{b2}) = \tau_\alpha] = 283$ K is close to the plateau temperature T_{b2}. Thus, DPG follows the T_{b2} rule, too.

4.1.3. Tripropylene glycol (TPG)

The PALS response of TPG measured over an extraordinary wide temperature range from 18 K up to 390 K is presented in the absolute temperature *T* and T_g^{PALS} normalized scale in Fig. 1. Similarly to the monomer and dimer, we observe an onset of the more rapid increase in the o-Ps lifetime at the first characteristic PALS temperature $T_g^{PALS} \sim$ 186 K followed by the weaker bend effect at the first characteristic liquid PALS temperature $T_{b1} = 231\ \text{K} = 1.24\ T_g^{PALS}$ and finally, finished by a dramatic crossover towards the plateau level at the second characteristic liquid PALS temperature $T_{b2} \sim 272\ \text{K} = 1.46\ T_g^{PALS}$. These relative PALS temperatures are comparable or slightly lower in comparison with PG and DPG, consistent with the higher fragility of TPG ($m_g = 74$) compared to PG and DPG [33].

The BDS spectra of TPG show that the trimer belongs to the class of Type B glass-formers [35]. The results of the analysis in terms of the sum of a CD and a CC function for the primary α relaxation and the secondary relaxation, respectively, are provided in Fig. 2c. Similarly as in the previous PG case, good fits of the BDS spectra could be achieved by including the CC term below 220 K. On the other hand, at $T > 220$ K the BDS spectra can be satisfactorily fitted when the CC term is neglected [33]. This finding seems to be related to the slighter change of slope of the PALS response above $T_{b1} \sim 231$ K in Fig. 1.

In Figs. 3 and 4, the relaxation map of TPG summarizing the primary α- and the secondary relaxation times is plotted together with the corresponding o-Ps lifetimes at both characteristic liquid PALS temperatures $\tau_3(T_{b1})$ and $\tau_3(T_{b2})$. The secondary peak is not detectable at T_{b1} so that the identity β temperature could not be determined. Next, the T_{b1} rule is found still to be valid. In Fig. 2c the equivalent frequency, $f_3(T_{b1})$, is indicated by the arrow, which reveals a transition from α-peak to secondary peak dominated response between 240 and 220 K, fully consistent with $T_{b1} = 231$ K, indicating that the onset of the secondary relaxation process could be responsible for the change of slope in the temperature dependent o-Ps lifetime of the TPG system, too.

With increasing temperature, the PALS response of the TPG sample develops into a very well pronounced plateau effect with some fine structure which occurs at the second characteristic liquid PALS temperature $T_{b2} = 272$ K — Fig. 1. From Fig. 3 it follows that the identity α temperature $T_\alpha[\tau_3(T_{b2}) = \tau_\alpha] = 277$ K is close to the plateau

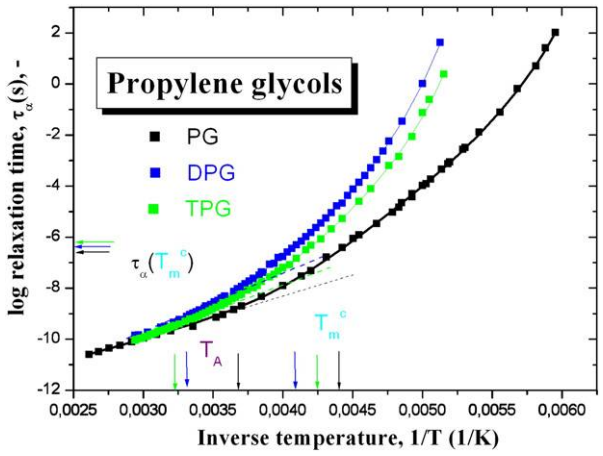

Fig. 5. Arrhenius plot of the structural relaxation times for PG, DPG and TPG [33] with the characteristic TOP temperatures, i.e., the characteristic Arrhenius temperatures: $T_A = 270$ K, 300 K and 310 K and the characteristic crossover TOP temperatures: $T_m^c = 227$ K, 244 K and 236 K. The lines represent the corresponding fits using the M-VFTH expression — Eq. (2).

temperature T_{b2}, so that, similarly as PG and DPG, TPG follows the T_{b2}rule, too.

4.2. Structural relaxation in terms of the TOP model and correlations of the PALS response with the further spectral and relaxation parameters of the structural relaxation in a series of PG's

Usually, the structural relaxation times τ_α as a function of temperature are parameterized by the Vogel–Fulcher–Tamman–Hesse (VFTH) equation. A Curie–Weiss (CW) law is often able to account for the temperature dependence of the structural relaxation strength, $\Delta\varepsilon_\alpha$, [33]. Alternatively, both quantities can be consistently described by the recently formulated two-order parameter (TOP) model of disordered glass-forming systems [54]. This model deals with disordered materials over a very wide temperature range assuming them to be composed of stable normal *liquid*-like regions, containing locally favored structures and their clusters, and frustrated metastable *solid*-like domains. The former type of region is supposed to play a dominant role in low viscosity (fast relaxing) liquids and at high temperatures that are above the thermodynamic transition temperature T_m^* from the ordinary, normal *liquid* to the frustrated *solid*-like state of a supercooled liquid. This temperature is expected to be close to the melting temperature T_m of the crystalline phase of crystallizing non-frustrated materials, which is often found to be close to the so-called Arrhenius temperature, T_A [54]. At this temperature, coming from above, the crossover from the Arrhenius- to non-Arrhenius type dynamical regime occurs. For example, in the case of strong glycerol, $T_A = 288$ K and $T_m = 293$ K; for fragile propylene carbonate $T_A = 218$ K and $T_m = 218$ K [6,54,55]. Thus, the dynamics of normal liquids is connected with the Arrhenius regime of the single main relaxation process [54]. Then, in the case of non-crystallizing compounds such as our *PG* systems T_A instead of T_m^* might be used. The TOP model considers the liquid–glass transition to be a consequence of the competition of ordering and of the frustration effects on ordering in *solid*-like domains. The proportion of the frustrated *solid*-like domains or islands in glass-formers grows with decreasing temperature through the supercooled liquid toward the glassy state. Thus, the dynamics exhibits the gradually heterogeneous and cooperative character that leads to the non-Arrhenius character of the viscosity or the structural relaxation. Finally, at very low temperatures below T_g, the *solid*-like domains are not able to reorganize and they should form the rigid glassy state. The phenomenological basis of the TOP model is given by the modified Vogel–Fulcher–Tamman–Hesse (M-VFTH) equation for the viscosity or relaxation time which is expected to be valid over a very wide temperature range including both the normal and supercooled liquid states [54]:

$$\tau_\alpha(T) = \tau_{\alpha\infty} \exp\left[E_\tau^* / RT\right] \exp\left[BF(T) / (T - T_0)\right] \quad (2)$$

Where $\tau(T)$ is the structural relaxation time, τ_∞ is the pre-exponent factor, E_τ^* is the activation energy above $T_m^* \sim T_A$, T_0 is the divergence temperature, B is the coefficient and $F(T)$ is a probability function for *solid*-like domains. The latter is defined as

$$F(T) = 1 / \left\{\exp\left[\kappa(T - T_m^c)\right] + 1\right\} \quad (3)$$

where κ describes the sharpness of the probability function and T_m^c is the characteristic TOP temperature, i.e., the critical temperature where the free energy of a crystallizing liquid is equal to that of the crystal $\Delta G_{lq} = \Delta G_{cr}$ or, in the general case of a non-crystallizing glass-formers, the free energy of a non-crystallizing liquid is equal to that of a solid: $\Delta G_{lq} = \Delta G_{sol}$.

Fig. 5 displays the fits of the structural relaxation time for the series of PG's over the whole measured temperature range in terms of the M-VFTH equation. Table 3 summarizes all the best fitting parameters of the M-VFTH equation.

Next, Fig. 6 presents tests of fitting of the relaxation strength of the structural relaxation, $\Delta\varepsilon_{CD}$, as a function of temperature in terms of the TOP model. The used functional form is: $\Delta\varepsilon_{CD} = a + bF(T)$ [54]. In all the cases, with an exception of the highest temperature value, a plausible fit is achieved suggesting that the structural relaxation strength, $\Delta\varepsilon_{CD}$, should be proportional to the fraction of the *solid*-like domains $F(T)$. In addition, the spectral width parameter of the structural relaxation, β_{CD}, as a function of temperature is also plotted. It mirrors the typical non-Debye behavior [22] with similar tendency towards an approximative saturation at a value below unity [57] roughly at around $T_X^{\beta_{CD}} \sim 270$ K, 280 K and 275 K for PG, DPG or TPG, respectively.

In the context of the PALS response in Fig. 1, the results of the TOP analysis in Figs. 5 and 6 and Table 2 can be discussed as follows:

First, from Fig. 5 it is seen that the Arrhenius regimes of all the PG's are consistent with the occurrence of the plateau effect in accord with the previous findings for polyphenylether (6PO) [17], glycerol [56] and propylene carbonate (Pc) [49].

Next, the characteristic TOP temperatures, T_m^c, of the PG's lie quite close to the first characteristic PALS temperatures in the PALS responses $T_{b1} = 218$ K, 232 K and 231 K, above which the slighter changes in slope of the τ_3–T plot occur. At the same time, these T_m^c's as well as T_{b1}'s values are quite close to the boundary temperatures for the existence of secondary process from the two-component analysis of the BDS spectra being 220 K for PG and TPG and 240 K for DPG [33].

Table 3
Fitting parameters of the M-VFTH equation for a series of PG's.

System	ΔT	T_A	$\log \tau_\infty$	E_τ	B	κ	T_m^c	T_0	$\log \tau\,(T_m^c)$
	[K]	[K]	[s]	[kcal/mol]	[K]	[1/K]	[K]	[K]	[s]
PG	168–383	270	14.95	7.6	423	0.0556	227.5	143	−6.5
DPG	195–340	300	15.88	9.6	398	0.0488	244	173	−6.3
TPG	194–340	310	16.09	9.4	357	0.0494	236	171	−6.2

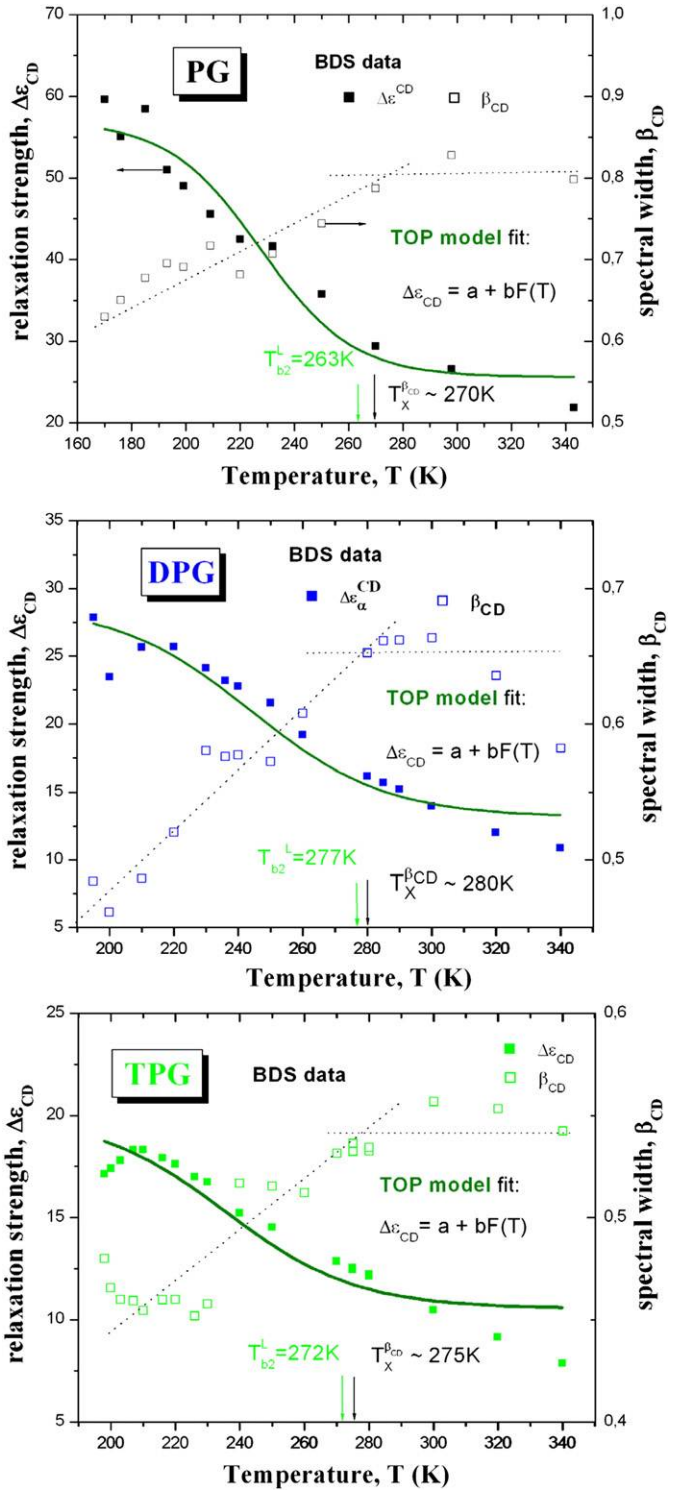

Fig. 6. Tests of the TOP model for the relaxation strength of the structural relaxation as a function of temperature in a form: $\Delta\varepsilon_{CD} = a + bF(T)$.The temperature dependence of the spectral width parameter, β_{CD}, is also included with the estimated crossover temperatures: $T_X^{\beta_{CD}}$ — see text.

According to the TOP model, in the *deeply* supercooled liquids below T_m^c the *solid*-like domain population dominates over the *liquid*-like one, resulting into the progressively increasing structural relaxation time after reaching the value of ~10^{-6} s towards the glass transition. Then, both the above-mentioned findings strongly suggest that the more rapid secondary process in the PG's should be related to the lower slope in the τ_3–T plots.

Further, Fig. 6 shows that the quasi-saturation effect in the structural relaxation strength, $\Delta\varepsilon_{CD}$, is accompanied by the saturation one in the spectral width parameter, β_{CD}, as a measure of the width of the structural relaxation time distribution. And moreover, that both the saturation tendencies seem to be related, at least approximately, to the quasi-saturation plateau in the respective PALS responses in the higher temperatures. The latter finding is in accord with our very recent detailed joint PALS and BDS study on another small-molecule glass-former: Pc [49]. These saturation tendencies seem to be consistent with the dominating action of the *liquid*-like domains at high T's. All these empirical facts strongly suggest that the structural relaxation process is closely connected with region III of the PALS response. Accordingly, the mechanism of the structural relaxation process within the TOP model consisting in dynamic disappearance and appearance of the *solid*-like domains [54] appears to be consistent with these results of relaxation mode identification analysis in Section 4.1. On increasing the temperature, the gradually increasing proportion of the slower parts of the α-relaxation time distribution participates in the PALS response resulting finally, in the pronounced bend effect at T_{b2} which lead to the T_{b2} rule being closely related to the maximum of the structural relaxation time distribution.

5. Conclusion

Combined PALS and BDS studies on a series of three small-molecule propylene glycols were performed. The two empirical rules concerning the mutual time scale relationships between the PALS and BDS data sets were confirmed and some novel correlations were revealed.

In particular, the T_{b2} rule concerning the dramatic change in the character of the PALS response at high temperatures is found to be valid, i.e., the plateau effect at T_{b2} is directly related to the mean structural relaxation process.

On decrease the temperature, the T_{b1} rule regarding the specific relationship between the o-Ps annihilation at ns-level time scale and the structural relaxation at μs-level is also fulfilled. The origin of this rule as manifested by the change of slope in $\tau_3(T)$ at T_{b1} appears to be related to the crossover from the primary α process to the secondary relaxation or excess wing controlling the reduced free volume hole expansion.

Thus, the gradual evolution of the PALS response in the supercooled liquid state from the smaller slope in the deeply supercooled state through the larger slope in the slightly supercooled one towards the plateau effect is closely related to the evolution of the BDS response from a superposed spectrum consisting of the secondary and primary processes at the lower temperatures to a spectrum dominated by the structural relaxation at the higher ones.

We conclude that the PALS response of the *PG* glass-formers reflecting their free volume is very closely related to the internal mobility above the glass–liquid transition in both the supercooled and normal liquid states. In other words, the PALS method measures the *effective* free volume microstructure modulated by the various types of the internal dynamics on the relevant time scale of the PALS method.

Acknowledgements

This work was supported by the VEGA Agency, Slovakia under grants no. 2/0014/09 (J.B.) and 2/7121/27 (O.Š.) and by the DAAD, Germany, grant no. D01260.

References

[1] P.G. Debenedetti, P.H. Stillinger, Nature 410 (2001) 259.
[2] For example: a series of review papers in Science 267 (1996)M.D. Ediger, C.A. Angell, S.R. Nagel, J. Phys. Chem. 100 (1996) 13 200.
[3] D.C. Champeney, R.B.N. Joarder, J.C. Dore, Mol. Phys. 58 (1986) 337; B. Frick, D. Richter, C. Ritter, Europhys. Lett. 9 (1989) 557.

[4] For example: J. Non-Cryst. Solids 131-133 (1991), 172-174 (1994), 235-237 (1998), 307-310 (2002) and 352 (2006).
[5] A.J. Barlow, J. Lamb, A.J. Matheson, Proc. Roy. Soc. A 292 (1966) 322.
[6] A. Schönhals, F. Kremer, A. Hofmann, E.W. Fischer, E. Schlosser, Phys. Rev. Lett. 70 (1993) 3459.
[7] F. Stickel, E.W. Fischer, R. Richert, J. Chem. Phys. 104 (1996) 2043.
[8] A. Alegria, J. Colmenero, P.O. Mari, I.A. Campbell, Phys. Rev. E 59 (1999) 6888.
[9] A. Schönhals, Europhys. Lett. 56 (2001) 815.
[10] T.G. Fox, P.J. Flory, J. Appl. Phys. 21 (1950) 581;
A.K. Doolittle, J. Appl. Phys. 22 (1951) 1031;
M.H. Cohen, D. Turnbul, J. Chem. Phys. 31 (1961) 1164;
G.S. Grest, M.H. Cohen, Adv. Chem. Phys. 48 (1981) 455.
[11] J.D. Ferry, Viscoelastic Properties of Polymers, 3 rd edWiley, New York, 1980;
J. Crank, G. Park (Eds.), Diffusion in Polymers, Academic Press, New York, 1968.
[12] G. Dlubek (Ed.), Encyclopedia of Polymer Science and Technology, Wiley & Sons, 2008.
[13] Y.C. Jean, P.E. Malton, D.M. Schrader (Eds.), Principles and Application of Positron and Positronium Chemistry, World Scientific, Singapore, 2003.
[14] J. Bartoš, in: R.A. Meyers (Ed.), Encyclopedia of Analytical Chemistry, Wiley&Sons, Chichester, 2000, p. 7968.
[15] S. Tao, J. Chem. Phys. 56 (1972) 5499;
M. Eldrup, D. Ligthbody, J.N. Sherwood, Chem. Phys. 63 (1981) 51;
H. Nakanishi, Y.C. Jean, S.J. Wang, in: S.C. Sharma (Ed.), Positron Annihilation Studies of Fluids, World Scientific, Singapore, 1988, p. 292.
[16] H.S. Landes, S. Berko, A.J. Zuchelli, Phys. Rev. 103 (1956) 828;
W. Brandt, S. Berko, W.W. Walker, Phys. Rev. 120 (1960) 1289;
E.L.E. Kluth, H. Clarke, B.G. Hogg, J. Chem. Phys. 40 (1964) 3180.
[17] W. Brandt, I. Spirn, Phys. Rev. 142 (1966) 231;
R.A. Pethrick, F.M. Jacobsen, O.E. Mogensen, M. Eldrup, J. Chem. Soc., Faraday Trans. 2 78 (1982) 287;
Y.C. Jean, T.C. Sandreczki, D.P. Ames, J. Polym. Sci., Part B: Polym. Phys. 24 (1986) 1247;
J. Krištiak, O. Šauša, P. Bandžuch, J. Bartoš, J. Radioanal. Nucl. Chem. 210 (1996) 563.
[18] J. Bartoš, O. Šauša, P. Bandžuch, J. Zrubcová, J. Krištiak, J. Non-Cryst. Solids 307–310 (2002) 417.
[19] R.A. Pethrick, F.M. Jacobsen, O.E. Mogensen, M. Eldrup, J. Chem. Soc., Faraday Trans. 2 76 (1980) 225;
J.R. Stevens, S.H. Chung, P. Horoyski, K.R. Jeffrey, J. Non-Cryst. Solids 172–174 (1994) 1207;
P. Bandžuch, J. Krištiak, O. Šauša, J. Zrubcová, Phys. Rev. B 61 (2000) 8784.
[20] D. Kilburn, J. Wawryszczuk, G. Dlubek, J. Pionteck, R. Hässler, M.A. Alam, Macromol. Chem. Phys. 207 (2006) 721;
J. Wu, G. Huang, Q. Pan, L. Qu, Y. Zhu, B. Wang, Appl. Phys. Lett. 89 (2006) 121904;
W. Salgueiro, A. Somoza, G. Consolati, F. Quasso, A. Marzocca, Phys. Status Solidi C 4 (10) (2007) 3771.
[21] P. Lunkenheimer, U. Schneider, R. Brand, A. Loidl, Contemp. Phys. 41 (2000) 15.
[22] F. Kremer, A. Schönhals (Eds.), Broadband Dielectric Spectroscopy, Springer, Berlin, 2002.
[23] J. Bartoš, D. Račko, O. Šauša, J. Krištiak, in: S.J. Rzoska, V. Mazur (Eds.), ARW NATO Series: Soft Matter under Exogenic Impacts, Fundamentals and Emerging Technologies, Springer-Verlag, Berlin, Germany, 2007, p. 113.
[24] J. Bartoš, O. Šauša, D. Račko, J. Krištiak, J.J. Fontanella, J. Non-Cryst. Solids 351 (2005) 2599.
[25] J. Bartoš, A. Alegría, O. Šauša, M. Tyagi, D. Gómez, J. Krištiak, J. Colmenero, Phys. Rev. E 76 (2007) 031503.
[26] J. Krištiak, J. Bartoš, K. Krištiaková, P. Bandžuch, Phys. Rev. B 49 (1994) 6601.
[27] P. Kirkegaard, M. Eldrup, O.E. Mogensen, N.J. Pedersen, Comput. Phys. Commun. 23 (1989) 307.
[28] U. Schneider, P. Lunkenheimer, A. Pimenov, R. Brand, A. Loidl, Ferroelectrics 249 (2001) 89.
[29] U. Schneider, P. Lunkenheimer, R. Brand, A. Loidl, Phys. Rev. E 59 (1999) 6924.
[30] R. Böhmer, B. Schiener, J. Hemberger, R.V. Chamberlin, Z. Phys. 99 (1995) 91.
[31] R. Böhmer, M. Maglione, P. Lunkenheimer, A. Loidl, J. Appl. Phys. 65 (1989) 901.
[32] A.A. Volkov, Yu.G. Goncharov, G.V. Kozlov, S.P. Lebedev, A.M. Prokhorov, Infrared Phys. 25 (1985) 369;
A.A. Volkov, G.V. Kozlov, S.P. Lebedev, A.M. Prokhorov, Infrared Phys. 29 (1989) 747.
[33] M. Köhler, P. Lunkenheimer, Z. Goncharov, R. Wehn, A. Loidl: J. Non.-Cryst. Solids 356 (2010) 529;
M. Köhler, PhD Thesis, Augsburg 2007.
[34] C. Leon, K.L. Ngai, C.M. Roland, J. Chem. Phys. 110 (1999) 11585.
[35] A. Kudlik, S. Benkhof, T. Blochowicz, T. Tschirwitz, E. Rössler, J. Mol. Struct. 479 (1999) 201.
[36] U. Schneider, R. Brand, P. Lunkenheimer, A. Loidl, Phys. Rev. Lett. 84 (2000) 5560;
P. Lunkenheimer, R. Wehn, Th. Riegger, A. Loidl, J. Non-Cryst. Solids 307–310 (2002) 336.
[37] K.L. Ngai, P. Lunkenheimer, C. Leon, U. Schneider, R. Brand, A. Loidl, J. Chem. Phys. 115 (2001) 1405.
[38] A.A. Pronin, M.V. Kondrin, A.G. Lyapin, V.V. Brazhkin, A.A. Volkov, P. Lunkenheimer, A. Loidl, Phys. Rev. E 81 (2010) 041503.
[39] R. Casalini, C.M. Roland, Phys. Rev. Lett. 91 (2003) 015702;
R. Casalini, C.M. Roland, Phys. Rev. B 69 (2004) 094202.
[40] J. Wuttke, M. Ohl, M. Goldammer, S. Roth, U. Schneider, P. Lunkenheimer, R. Kahn, B. Rufflé, R. Lechner, M.A. Berg, Phys. Rev. E 61 (2000) 2730.
[41] S. Pawlus, S. Hensel-Bielowka, M. Paluch, R. Casalini, C.M. Roland, Phys. Rev. B 72 (2005) 064201.
[42] K. Grzybowska, A. Grzybowski, J. Ziolo, S.J. Rzoska, M. Paluch, J. Phys. Condens. Matter 19 (2007) 376105.
[43] G.P. Johari, M. Goldstein: J. Chem. Phys. 53 (1970) and 55 (1971) 4245.
[44] K.L. Ngai, M. Paluch, J. Chem. Phys. 120 (2004) 857.
[45] D.W. Davidson, R.H. Cole, J. Chem. Phys. 19 (1951) 1484.
[46] K.S. Cole, R.H. Cole, J. Chem. Phys. 9 (1941) 341.
[47] J.C. Dyre, N.B. Olsen, Phys. Rev. Lett. 91 (2003) 155703;
K. Grzybowska, A. Grzybowski, M. Paluch, J. Chem. Phys. 128 (2008) 134904;
Y.E. Ryabov, A. Puzenko, Y. Feldman, Phys. Rev. B69 (2004) 014204.
[48] G. Consolati, Appl. Phys. Lett. 88 (2006) 111902.
[49] K.L. Ngai, L.R. Bao, A.F. Yee, C.L. Soles, Phys. Rev. Lett. 87 (2001) 215901;
J. Bartoš, V. Majernik, M. Iskrová, O. Šauša, J. Krištiak, P. Lunkenheimer, A. Loidl, J. Non-Cryst. Solids 356 (2010) 794;
G. Dlubek, M.Q. Shaikh, K. Rätzke, M. Paluch, F. Faupel, J. Phys. Condens. Matter 22 (2010) 235104.
[50] J. Bartoš, J. Krištiak, J. Non-Cryst. Solids 235 (1998) 293.
[51] P.K. Dixon, L. Wu, S.R. Nagel, B.D. Williams, J.P. Carini, Phys. Rev. Lett. 65 (1990) 1108.
[52] K.L. Ngai, J. Phys. Condens. Matter 15 (2003) S1107.
[53] D. Račko, R. Chelli, G. Cardini, S. Califano, J. Bartoš, Theor. Chem. Acc. 118 (2007) 443.
[54] H. Tanaka: J. Phys. Condens. Matter 10 (1998) L207; H. Tanaka: J. Phys. Condens. Matter 11 (1999) L159; H. Tanaka: J. Chem. Phys. 111 (1999) 3163 and 3175; H. Tanaka: J.Non-Cryst. Solids 351 (2005) 3371, 3385 and 3396
[55] P. Lunkenheimer, A. Loidl, Chem. Phys. 284 (2002) 205.
[56] J. Bartoš, Mater. Sci. Forum 607 (2009) 48.
[57] U. Schneider, R. Brand, P. Lunkenheimer, A. Loidl, Eur. Phys. J. E 2 (2000) 67.